



## Numerical simulations of chilling and freezing processes applied to bakery products in irregularly 3D geometries

María V. Santos<sup>a,b</sup>, Victoria Vampa<sup>b</sup>, Alicia Califano<sup>a,\*</sup>, Noemí Zaritzky<sup>a,b</sup>

<sup>a</sup> Centro de Investigación y Desarrollo en Criotecología de Alimentos (CIDCA), CONICET-La Plata, Facultad de Ciencias Exactas, Universidad Nacional de La Plata, 47 y 116, La Plata 1900, Argentina

<sup>b</sup> Facultad de Ingeniería, Universidad Nacional de La Plata, Argentina

### ARTICLE INFO

#### Article history:

Received 26 December 2009

Received in revised form 5 March 2010

Accepted 13 March 2010

Available online 20 March 2010

#### Keywords:

Finite element method

Numerical simulations

Freezing

Chilling

Irregular domains

Kirchhoff transformation

Enthalpy

Bakery products

### ABSTRACT

Finite element algorithms implemented in numerical codes were developed by the authors for irregular 3D food systems, to simulate: (i) the chilling process considering domains of different thermo-physical properties, and (ii) the freezing operation using a combined enthalpy and Kirchhoff transformation. The specific heat of the food materials were measured using Differential Scanning Calorimetry and the heat transfer coefficients of the low temperature equipments were determined; this information was further used as inputs in the model.

The numerical solutions, previously validated with analytical solutions, were compared to experimental time–temperature curves using different bakery products for chilling and freezing. A good agreement between measurements and model predictions were obtained in all cases. In the complex freezing process the application of the enthalpy–Kirchhoff formulation decreased the computational efforts improving the rate of convergence and the execution speed with respect to the commercial softwares. The codes were applied to determine the required time–temperature conditions for food chilling and freezing.

© 2010 Elsevier Ltd. All rights reserved.

### 1. Introduction

The bakery industry has been deeply changed due to developing technologies. The chilling and freezing processes incorporated at different steps during the manufacturing of bakery products, has enabled the introduction of semi-processed goods to the market. Several technologies consist of dough refrigeration, freezing of a fermented, pre-fermented dough, or partially baked dough, and freezing of a completely baked product (Ribotta et al., 2006).

The “Bake-Off Technologies” (BOT) consist in the manufacturing of the dough at an industrial scale and the distribution to the different commercial-shops. The idea behind this process is to give consumers a high quality product with a better level of freshness, since the final stage of the preparation is carried out in small shops where the product is baked. The market share of BOT is increasing at an estimated 10% per year and there is a considerate transfer of the traditional baking towards the BOT manufacturing (Le Bail and Goff, 2008).

Normally these semi-processed products cannot be properly assimilated to an object of regular geometry, which is a very important aspect to be considered when trying to numerically simulate the chilling and freezing processes. Examples of typical

bakery products that implemented the BOT are croissants, pastries, and ethnic food. Croissants are well-known pastry products in almost every country. “Empanadas” is a typical food eaten in different South American countries quite similar to Cornish pastries, where small circles (11 cm of diameter) of pastry dough are topped with different fillings and folded over into a half-moon, which can be later fried or baked (Lorenzo et al., 2009). A traditional filling is made of cooked minced lean meat. The pastry edges are firmly pressed together to seal the filling and fluted. “Empanada” is therefore a heterogeneous product made of two different materials (meat and dough). Before the baking or cooking stage these products can either be chilled and/or frozen. This kind of product has an irregular 3D geometry that must be considered to predict cooling times and find optimal process conditions.

A possible approach to obtain the actual shape of an irregular foodstuff is to use Computer Aided Design (CAD), where the objects shape is generated in a specific 3D drawing Software such as Solidworks. These 3D geometry images can be later imported to a mesh generator for the discretization of the continuous 3D domain.

The finite element method is an established formulation for the solution of heat conduction problems (Cleland et al., 1984) such as chilling and freezing. It has the great advantage that it can deal better with problems where the object has an irregular geometry with defined regions (domains) of different composition (Arce et al., 1983; Pham, 2008).

\* Corresponding author. Tel./fax: +54 221 425 4853.

E-mail address: [anc@quimica.unlp.edu.ar](mailto:anc@quimica.unlp.edu.ar) (A. Califano).

## Nomenclature

$T$	temperature, vector of nodal temperatures (°C)
$CG$	global capacitance matrix
$C_p$	specific heat J/(kg °C)
$C_{p_{ap}}$	apparent specific heat J/(kg °C)
$E$	Kirchhoff function (W/m)
$FG$	global force vector
$N$	vector containing the shape functions
$N_j$	shape function $j$
$h$	surface heat transfer coefficient (W/m <sup>2</sup> °C)
$H$	volumetric enthalpy (J/m <sup>3</sup> )
$k$	thermal conductivity (W/m °C)
$KG$	global conductance matrix
$MG$	global convective matrix
$t$	time (s)
$T_{ext}$	external fluid temperature (°C)
$T_f$	initial freezing temperature (°C)
$T_{ref}$	reference temperature (°C)

<i>Greek letters</i>	
$\Delta t$	time increment (s)
$\delta\Omega$	surface of the domain
$\varepsilon$	residual (W/m <sup>3</sup> )
$\rho$	density (kg/m <sup>3</sup> )
$\Omega$	domain

<i>Subscripts</i>	
0	initial
1, 2	domain
$e$	element
$e_1$	border element
$w$	water

<i>Superscript</i>	
$t$	transpose

During the freezing process, which involves the phase change of water into ice in the food product, the thermo-physical properties such as specific heat, thermal conductivity, and density undergo abrupt changes due to the latent heat release. The system is then established as a highly non-linear mathematical problem. Several techniques were applied to deal with the large latent heat release when using the finite element method. One of the traditional methods is the use of the apparent specific heat, where the sensible heat is merged with the latent heat to produce a specific heat curve with a large peak around the freezing point, that can be considered a quasi-delta-Dirac function with temperature (depending on the amount of water in the food product). The abrupt change in the apparent specific heat curve requires several iterations for each time step and usually destabilizes the numerical solution. In some commercial simulation softwares that implement the finite element method, such as COMSOL, the use of the apparent specific heat is the only method available (Pham, 2008). Many authors have done approximations by “softening” the peak curve in order to obtain some convergence of the method, modifying the shape of the apparent specific heat curve while maintaining the total latent heat constant. However, this softening method is not recommended, because the actual temperature range around the freezing zone, is altered becoming wider than the actual temperature freezing range.

The implementation of the enthalpy method, which can be obtained through the integration of the specific heat with temperature (Comini et al., 1974; Mannapperuma and Singh, 1988, 1989; Pham, 2008), and the Kirchhoff function, which is the integral of the thermal conductivity, allows the reformulation of the heat transfer differential equation into a transformed partial differential system with two mutually related dependent variables  $H$  (enthalpy) and  $E$  (Kirchhoff function) (Scheerlinck et al., 2001). Works combining the enthalpy and Kirchhoff transformations are scarce in the literature, even though it generates great advantages to the resolution of the phase change problem, since all the non-linearities are incorporated into a single functional relationship between the volumetric specific enthalpy and the thermal conductivity integral (Fikiin, 1996, 1998; Scheerlinck et al., 1997). Combining both transformations helps to avoid inaccuracies and/or divergence of the numerical method, caused by the latent heat peak release and the jump of the thermal conductivity at the phase transition, with the great numerical advantage of minimizing the execution speed of the program, since the resulting finite element matrices are constant.

The goals of this work are:

- (1) To develop a code that simulates: (a) the chilling process in irregular 3D food systems with domains of different thermo-physical properties using the finite element method; (b) the freezing process of an irregular shaped food using a combined enthalpy and Kirchhoff transformation method.
- (2) To measure the specific heat of the bakery products by Differential Scanning Calorimetry (DSC) and the heat transfer coefficients of the low temperature equipments, incorporating these data in the numerical model.
- (3) To validate the numerical solutions with analytical results and to compare the numerical simulations with experimental data using different bakery products for the chilling and freezing processes.

## 2. Materials and methods

### 2.1. Finite element simulation during the chilling process

The differential heat equation that governs the cooling process without phase change in a three dimensions is as follows:

$$\rho C_p \frac{\partial T}{\partial t} = \nabla \cdot (k \nabla T) \quad \text{in } \Omega \quad (1)$$

In the case of constant thermal conductivity (such as in the chilling process):

$$\nabla \cdot (k \nabla T) = k \left( \frac{\partial^2 T}{\partial x^2} + \frac{\partial^2 T}{\partial y^2} + \frac{\partial^2 T}{\partial z^2} \right) \quad (2)$$

The equation is valid in the domain  $\Omega$ , where  $T$  is the temperature,  $k$  is the thermal conductivity,  $C_p$  the specific heat, and  $\rho$  the density (Carslaw and Jaeger, 1959). The initial and boundary conditions are:

$$T = T_0 \quad t = 0 \quad \text{in } \Omega \quad (3)$$

$$-k \left( \frac{\partial T}{\partial x} \cdot n_x + \frac{\partial T}{\partial y} \cdot n_y + \frac{\partial T}{\partial z} \cdot n_z \right) = h(T - T_{ext}) \quad t \geq 0 \quad \text{in } \delta\Omega \quad (4)$$

where  $\delta\Omega$  is the domain of the convective interface which corresponds to external surface in contact with the cooling air,  $n_x$ ,  $n_y$ , and  $n_z$  are the normal outward vector components,  $T_{ext}$  is the

external air temperature;  $T_0$  is the initial food temperature and  $h$  is the surface heat transfer coefficient.

In order to solve the governing heat transfer equation a numerical finite element algorithm was developed. The temperature distribution at any point in the domain was approximated by using interpolating functions ( $N_j$ ) and the node temperatures in the given element.

After applying Galerkin weighted residual method (Bathe, 1996; Zienkiewicz and Taylor, 1994a,b), the following system is obtained:

$$\left[ \sum_e \int_{\Omega_e} N^t \rho C_p N d\Omega \right] \dot{T} + \left[ \sum_{e_1} \int_{\delta\Omega_{e_1}} N^t h N d\delta\Omega_{e_1} + \sum_e \int_{\Omega_e} B^t k B d\Omega \right] T = \left[ \sum_{e_1} \int_{\delta\Omega_{e_1}} N^t h T_{ext} d\delta\Omega_{e_1} \right] \quad (5)$$

where  $N$  is the vector of dimensions  $[1 \times 4]$  containing the shape functions ( $N_j$ ) with  $j = 1-4$  for the reference tetrahedron element,  $N^t$  is the transpose vector (dimension  $4 \times 1$ ),  $e$  refers to the finite elements,  $e_1$  refers to the boundary elements,  $\Omega_e$  is the integration domain,  $\delta\Omega_{e_1}$  is the boundary integration domain. The matrix  $B$  (dimension  $3 \times 4$ ) is defined as follows:

$$B = \begin{bmatrix} N_{1x} & N_{2x} & N_{3x} & N_{4x} \\ N_{1y} & N_{2y} & N_{3y} & N_{4y} \\ N_{1z} & N_{2z} & N_{3z} & N_{4z} \end{bmatrix}$$

where  $N_{ix} = \frac{\partial N_i}{\partial x}$ ,  $N_{iy} = \frac{\partial N_i}{\partial y}$  and  $N_{iz} = \frac{\partial N_i}{\partial z}$  for  $i = 1-4$ .

Eq. (5) can be written as follows:

$$CG \cdot \dot{T} + KG \cdot T = FG \quad (6)$$

where

$$CG = \sum_{e=1}^n \int_{\Omega_e} (N^t \rho C_p N) d\Omega_e \quad (7)$$

$$KG = \sum_{e=1}^n \int_{\Omega_e} (B^t k B) d\Omega_e + \sum_{e_1=1}^{ne_1} \int_{\delta\Omega_{e_1}} (N^t h N) d\delta\Omega_{e_1} \quad (8)$$

$$FG = \sum_{e_1=1}^{ne_1} \int_{\delta\Omega_{e_1}} (N^t h T_{ext}) d\delta\Omega_{e_1} \quad (9)$$

$CG$  is the global capacitance matrix,  $KG$  is the global conductance matrix, and  $FG$  the global force vector.  $T$  is the vector that represents the temperature values at the node points, and  $\dot{T}$  represents the  $\frac{dT}{dt}$ . This semi-discrete problem (Eq. (6)) is a system of stiff ordinary differential equations. This system was solved using the standard Matlab routines ordinary differential equations (ODE) (Shampine and Reichelt, 1997), specifically ODE15s subroutine was applied which is an automatic algorithm for stiff problems; it was implemented using an implicit Backward Differentiation Formula (BDF) of order 5, as recommended by Scheerlinck et al. (2001). Due to the computational cost, the choice of the time step scheme is very important. In this regard, the use of ODE schemes is efficient since they have an automatic control time-step size. As the order of the BDF increases, the stability region is reduced, however in all the cases studied in this work, results showed both stability and accuracy, with minimum computational efforts.

## 2.2. Finite element simulation during the freezing process

During the phase change transition in the freezing process the thermo-physical properties are strongly dependent on temperature and Eq. (2) is no longer valid. This constitutes a highly non-linear mathematical problem that can be written as:

$$\rho(T) C_p(T) \frac{\partial T}{\partial t} = \nabla \cdot (k(T) \nabla T) \quad \text{in } \Omega \quad t \geq 0 \quad (10)$$

By performing the following change of variables:

$$H(T) = \int_{T^*}^T \rho(T) \cdot C_p(T) dT \quad (11)$$

$$E(T) = \int_{T^*}^T k(T) dT \quad (12)$$

where  $H$  is defined as the volumetric specific enthalpy (Comini et al., 1990),  $E$  is the Kirchhoff function that represents the thermal conductivity integral (Comini et al., 1990; Fikiin, 1996), and  $T^*$  is a reference temperature that corresponds to a zero value of  $H$  and  $E$ . By combining Eqs. (10)–(12), and the initial and boundary conditions represented by Eqs. (3) and (4) the following equations were obtained:

$$\frac{\partial H}{\partial t} = \nabla^2 E \quad \text{in } \Omega \quad t \geq 0 \quad (13)$$

$$-(\nabla E) \cdot n = h \cdot (T - T_{ext}) \quad \text{in } \delta\Omega \quad t \geq 0 \quad (14)$$

$$H = H_0 \quad t = 0 \quad (15)$$

Defining the residual as:

$$r = \frac{\partial H}{\partial t} - \nabla^2 E \quad (16)$$

Applying the weighted residual method,

$$\int_{\Omega} N^t \left( \frac{\partial H}{\partial t} - \nabla^2 E \right) d\Omega = 0 \quad (17)$$

Using the differentiation rule, the term  $-\nabla^2 E$  can be written as  $-\nabla \cdot (\nabla E) + \nabla N^t \cdot \nabla E$ . After applying the divergence theorem, the following equation is obtained

$$\int_{\Omega} N^t \frac{\partial H}{\partial t} d\Omega - \int_{\delta\Omega} N^t \nabla E \cdot n d\delta\Omega + \int_{\Omega} \nabla N^t \cdot \nabla E d\Omega = 0 \quad (18)$$

The boundary condition (14) was incorporated into the variational formulation in the second term of Eq. (18) leading to:

$$\int_{\Omega} N^t \frac{\partial H}{\partial t} d\Omega + \int_{\delta\Omega} N^t h (T - T_{ext}) d\delta\Omega + \int_{\Omega} \nabla N^t \cdot \nabla E d\Omega = 0 \quad (19)$$

$$\int_{\Omega} N^t \frac{\partial H}{\partial t} d\Omega + \int_{\delta\Omega} N^t h T d\delta\Omega + \int_{\Omega} \nabla N^t \cdot \nabla E d\Omega = \int_{\delta\Omega} N^t h T_{ext} d\delta\Omega \quad (20)$$

Rearranging, and after applying Galerkin method:

$$CG \cdot \frac{dH}{dt} + FG \cdot T(H) + KG \cdot E(H) = m \quad (21)$$

where

$$CG = \sum_{e=1}^{ne} \int_{\Omega_e} (N^t N) d\Omega_e \quad \text{is the global capacitance matrix}$$

$$KG = \sum_{e=1}^{ne} \int_{\Omega_e} (B^t B) d\Omega_e \quad \text{is the global conductance matrix}$$

$$FG = \sum_{s=1}^{ns} \int_{\Omega_s} (N^t h N) d\delta\Omega_s \quad \text{is the global convection matrix}$$

$$m = \sum_{s=1}^{ns} \int_{\delta\Omega_s} (N^t h T_{ext}) d\delta\Omega_s \quad \text{is the global thermal load vector}$$

$H$ ,  $E$ , and  $T$  are the nodal values of enthalpy, the Kirchhoff function, and temperature, respectively.

It can be observed that the thermal properties of the foodstuffs are not present in the calculations of the matrices; therefore these matrices need to be calculated only once, which reduces the computer time significantly. If the surface heat transfer coefficient is considered constant during the process,  $FG$  and  $m$  also remain constant.

Eq. (21) is also a system of ordinary differential equations with three unknown variables,  $H$ ,  $E$ , and  $T$  that are interrelated through non-linear algebraic functions ( $H(T)$ ,  $E(T)$ ,  $H(E)$ ,  $T(H)$ ,  $T(E)$ ,  $E(H)$ ). Incorporating the functions  $E(H)$  and  $T(H)$  in Eq. (21) the system can be rewritten as:

$$\frac{dH}{dt} = f(H) \quad (22)$$

The system was solved using the standard Matlab routines ordinary differential equations (ODE) as described in Section 2.1.

In order to obtain the temperatures, the function  $T(H)$  was used, since the solution is given in enthalpy values at the mesh nodes.

### 2.3. Mesh generation

The 3D representation of the irregular bakery products were obtained using Computer Aided Design (CAD) in Solidworks. These files were imported into a mesh generator, discretizing domain into tetrahedral elements.

### 2.4. Experimental procedure

#### 2.4.1. Materials

Two different bakery products, “empanada” (Cornish pastry) and “croissants” were used to verify the computer code. The semi-elaborated product Cornish pastry was prepared using cooked minced lean beef and dough circles (2 mm thick). With the object of maintaining the exact irregular shape of the product for each experiment, a plastic cast was used; half of the dough disk was placed in the cast with the half moon shape hole (leaving the other half loose but still attached to the dough disk) then filled with cooked ground beef ( $66 \pm 3\%$  water content) and finally sealed with the other half of the dough disk, pressing firmly to seal the interior filling. Once the Cornish pastry was prepared it was placed in a cold chamber at  $5^\circ\text{C}$ , recording the temperature in the product by inserting several copper–constantan thermocouples connected to a data acquisition system (Testo 175, Testo AG, Germany).

The dough composition was 47% carbohydrates, 30% water, 15% lipids, 6% protein, and 2% fiber, as given by the producer.

Croissants were elaborated using a 2 mm thick dough which was cut into isosceles triangles (15 cm base, 21 cm height) and further rolled into the croissants shape. They were selected to analyze the freezing process. Several samples were placed in a tunnel freezer with circulating air in order to obtain similar industrial operating conditions. The temperature curves of the samples at several points inside the product were recorded using a temperature acquisition device (Testo 175, Testo AG, Germany). The cooling air velocity in the tunnel freezer was measured using a hot wire anemometer (TSI model 1650).

#### 2.4.2. Experimental determination of the food properties

Specific heat of the dough samples and the filling of the Cornish pastry was determined using a Differential Scanning Calorimeter (DSC) TA Instruments, New Castle, Delaware, USA model Q100 controlled by a TA 5000 module with a quench cooling system under a nitrogen atmosphere at 20 mL/min.

Samples of cooked minced lean beef (filling) and the dough samples were prepared before the analysis and enclosed in a sealed aluminum pans. An empty pan was used as a reference sample. A heating rate of  $2^\circ\text{C}/\text{min}$  was used with an isothermal period of

10 min at  $-50$  and  $100^\circ\text{C}$ . In order to measure the specific heat of each material three scans have to be made: one for the sample, one for a standard (sapphire), and one for the empty sample pan. In all three scans the reference holder contains an empty pan. The specific heat can be calculated following the ASTM E1269 and McNaughton and Mortimer (1975) instructions.

The moisture contents (%) of the meat and the dough products were determined by drying triplicate samples in an oven at  $80^\circ\text{C}$  until reaching constant weight.

The density (mass/volume) of the dough component at room temperature ( $20^\circ\text{C}$ ) was calculated using the method described by Baik et al. (2001) where a sample of dough is cut into a regular geometry, whose volume can be calculated using the dimensions measured by a caliber instrument. The volume of the cooked minced lean beef was measured using a Seed Replacement Method, previously wrapping the minced meat in a plastic film in order to avoid product loss.

The initial freezing temperature  $T_f$  of the dough was experimentally determined by using thermocouples inserted in a dough cylinder that was placed in the tunnel freezer at  $-20^\circ\text{C}$ . From the cooling curves  $T_f$  was measured using the tangent method described in Fennema et al. (1973).

#### 2.4.3. Determination of the surface heat transfer coefficient ( $h$ )

In order to estimate the surface heat transfer coefficient the transient method was used; the numerical solution of heat conduction equation is the most appropriate method when dealing with heterogeneous foodstuffs, complex 3D geometries or variable boundary conditions (Arce et al., 1983; Rahman et al., 2005).

Two solid bodies of the same shape as the bakery products (Cornish pastry and croissant) were made in acrylic (prototypes). In order to build the object with the exact shape as the foodstuff the CAD files were imported into a PC-based computer numerical control drilling machine. The adopted values of the thermo-physical properties of the acrylic resin at the studied range ( $-40$  to  $40^\circ\text{C}$ ) were:  $k = 0.2075 \text{ W/m}^\circ\text{C}$ ,  $C_p = 1464 \text{ J/kg}^\circ\text{C}$ ,  $\rho = 1180 \text{ kg/m}^3$  (given by the producer, Acrilico Paolini S.A.I.C.); they were considered constant in the temperature interval since there is no phase change transition. The Cornish pastry prototype was placed in the cooling chamber and the croissant prototype in the tunnel freezer, at the same operating conditions as the industrial bakery processing. The temperature evolution at the center and surface of each prototype, as well as the external cooling air temperature was recorded by means of an acquisition system using copper–constantan thermocouples. Different heat transfer coefficients were used to simulate temperature profiles; experimental and predicted temperatures for each proposed  $h$  coefficient were compared. The heat transfer coefficient that minimized the residual sum of squares (RSS) given by Eq. (23) was selected.

$$\text{RSS} = \sum (T_{\text{exp}} - T_{\text{pred}})^2 \quad (23)$$

The surface heat transfer coefficients for each system (chilling or freezing) were then compared with correlations given in literature.

## 3. Results and discussion

### 3.1. Chilling of irregular 3D heterogeneous foodstuffs

Fig. 1a–c shows a photograph of the actual product (Cornish pastry) and the spatial representation of the mesh generated by the software Solidworks including the visualization of the interior domain discretized into tetrahedral elements. The interior domain consists of the cooked minced lean beef and the outer domain is the thin layer (2 mm thick) of dough.

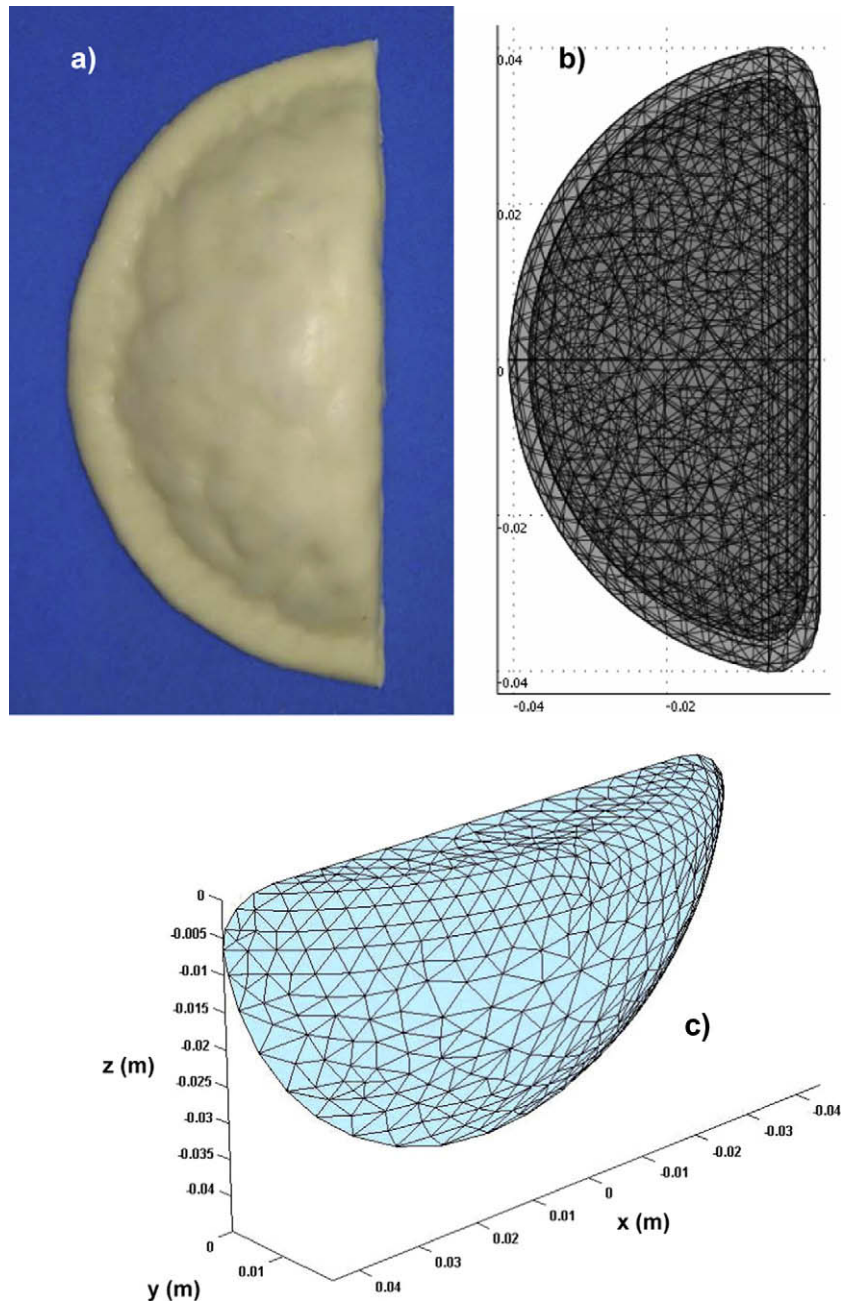


**Fig. 1.** (a) Digital photograph of the Cornish pastry bakery product; (b) and (c) spatial representation of the irregularly shaped body using tetrahedral elements, in the meat filling (inner domain) and dough (external domain).

### 3.1.1. Thermo-physical properties of the product

The experimental water content of the cooked meat filling was  $66 \pm 3\%$ ; the density above  $0\text{ }^{\circ}\text{C}$  was  $604\text{ kg/m}^3$ , and the thermal conductivity was estimated using the following equation (Sweat, 1975):

$$k = 0.08 + 0.52 \cdot x_w \quad (24)$$

where  $x_w$  corresponds to the moisture content of the meat component. The obtained thermal conductivity value used for the chilling process of the cooked minced lean beef was  $0.433\text{ W/m }^{\circ}\text{C}$ .

The specific heat measured by DSC for both components (meat and dough) did not show significant changes at the studied range ( $0\text{--}25\text{ }^{\circ}\text{C}$ ) and average values of  $2951 \pm 39\text{ J/kg }^{\circ}\text{C}$  for meat filling, and  $1938.5 \pm 1\text{ J/kg }^{\circ}\text{C}$  for the dough, were used.

The dough used for the preparation of Cornish pastry was of a commercial type with a composition of 47% carbohydrates, 30% water, 15% fat, 6% protein and 2% fiber, as given by the producer. The experimental water content for the dough was  $30 \pm 2.5\%$ , with a measured density of  $\rho = 1220.9\text{ kg/m}^3$ . The thermal conductivity was calculated using the formula given by Choi and Okos (1986), and was considered independent of temperature in the range  $0\text{--}25\text{ }^{\circ}\text{C}$ ; the average value used was  $k = 0.3278\text{ W/m }^{\circ}\text{C}$  (SEM =  $0.0001\text{ W/m }^{\circ}\text{C}$ ), which was in agreement with  $k$  values reported in literature for un-leavened dough (Baik et al., 2001).

### 3.1.2. Surface heat transfer coefficient

The surface heat transfer coefficient ( $h$ ) that minimized the RSS (Eq. (23)) for the chilling process of the irregularly shaped Cornish pastry in the cooling chamber was  $5.5\text{ W/m}^2\text{ }^{\circ}\text{C}$ . The surface heat

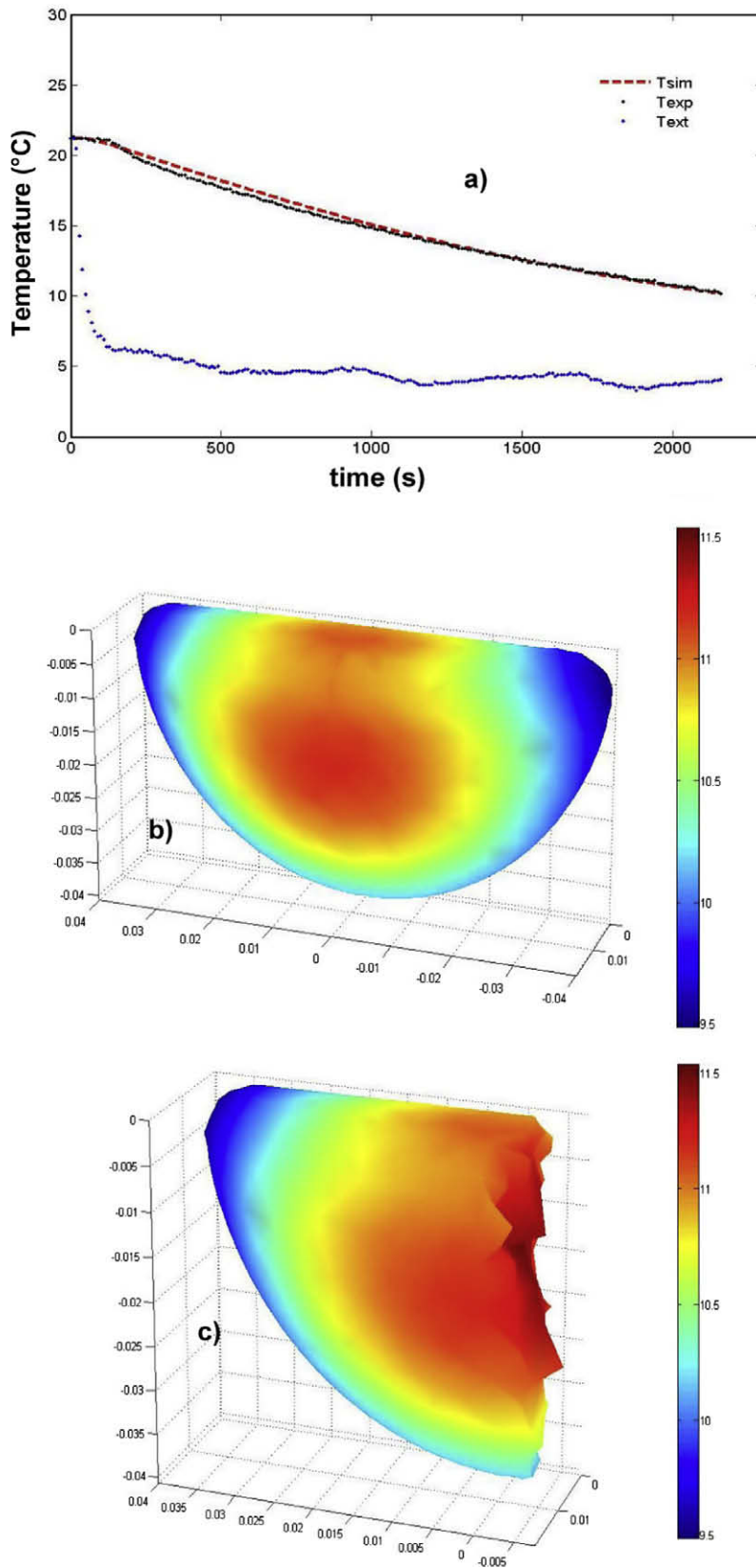


**Fig. 2.** (a) Numerical predictions (---) and experimental (—) time–temperature curves at  $(x, y, z) = (0, 0.10, -0.01)$  (coordinates in m), during the chilling of Cornish pastry in a cold chamber with external fluid temperature  $T_{ext} = 5$  °C. Initial product temperature 21.8 °C,  $h = 5.5$  W/m<sup>2</sup> °C; temperature distribution in the product after being cooled during 5 min (b) at the surface, (c) at the symmetry plane.

transfer coefficient  $h$  was estimated using literature correlations for immersed objects in a natural air convection chamber (Earle,

1988; Nesvadba, 2008) which lead to  $h$  values ranging between 5 and 20 W/m<sup>2</sup> °C. The experimental procedures in the cooling

**Table 1**  
Chilling times (min) for different values of  $T_{ext}$  and  $h$  (surface heat transfer coefficients).

$T_{ext}$ (°C)	Surface heat transfer coefficient $h$ (W/m <sup>2</sup> °C)				
	5	10	15	20	40
0	46.6	25.6	18.5	14.8	9.1
2	59.5	32.3	23.1	18.5	11.3
3	70.3	38.0	27.1	21.6	13.2

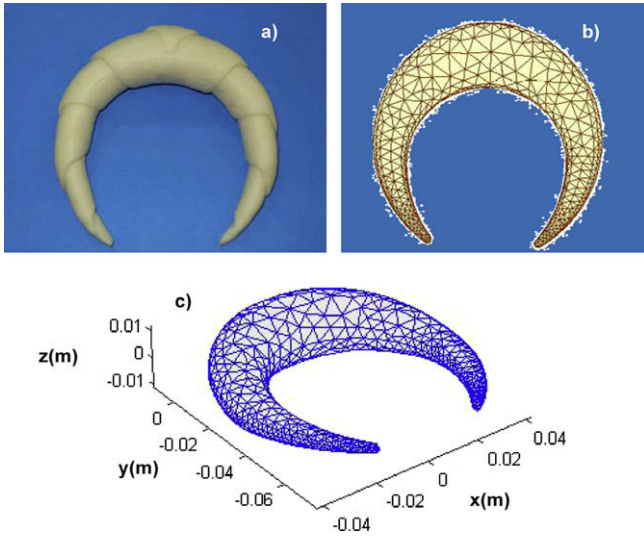


**Fig. 3.** (a) Digital photograph of the croissant; (b) and (c) 3D discretization of the bakery product.

chamber were made under these conditions, with a low circulation of the air, therefore a natural convection can be assumed. The predicted values of  $h$  for the chilling process in Cornish pastry satisfactorily agreed with the literature values considering an object submerged in a fluid.

**3.1.3. Validation of the numerical method for the chilling process and comparison with experimental results**

The numerical model which consisted in a pre-processing, main, and post-processing routines, were all coded in Matlab language. The codes implemented in 3D geometries were validated using the analytical solution of the heat conduction equation with convective boundary conditions for a sphere and a cylinder (Welty, 1974; Carslaw and Jaeger, 1959). The accuracy and convergence of the numerical predictions were corroborated, calculating the difference between numerical and analytical solutions (Santos et al., 2008). The numerical results were in agreement with the analytical solutions for both systems studied (sphere and cylinder), therefore the numerical code was considered theoretically validated.

Furthermore the codes were compared with experimental results during the chilling process for an irregularly 3D shaped food system with heterogeneous composition (Cornish pastries).

Fig. 2a shows the experimental and predicted temperatures at point  $(x, y, z) = (0, 0.10, -0.01)$  of the Cornish pastry (initial temperature = 21.8 °C) chilled with air at 5 °C in a cold chamber. As can be seen the numerical model satisfactorily predicts the time-temperature evolution of the chilling process. For all experiments the infinite norm (maximum value of the absolute error,  $\max |T_{exp} - T_{pred}|$ ) was less than 1.3 °C.

Fig. 2b shows the temperature distribution of the product after 5 min in the cooling chamber. Fig. 2c visualizes the interior

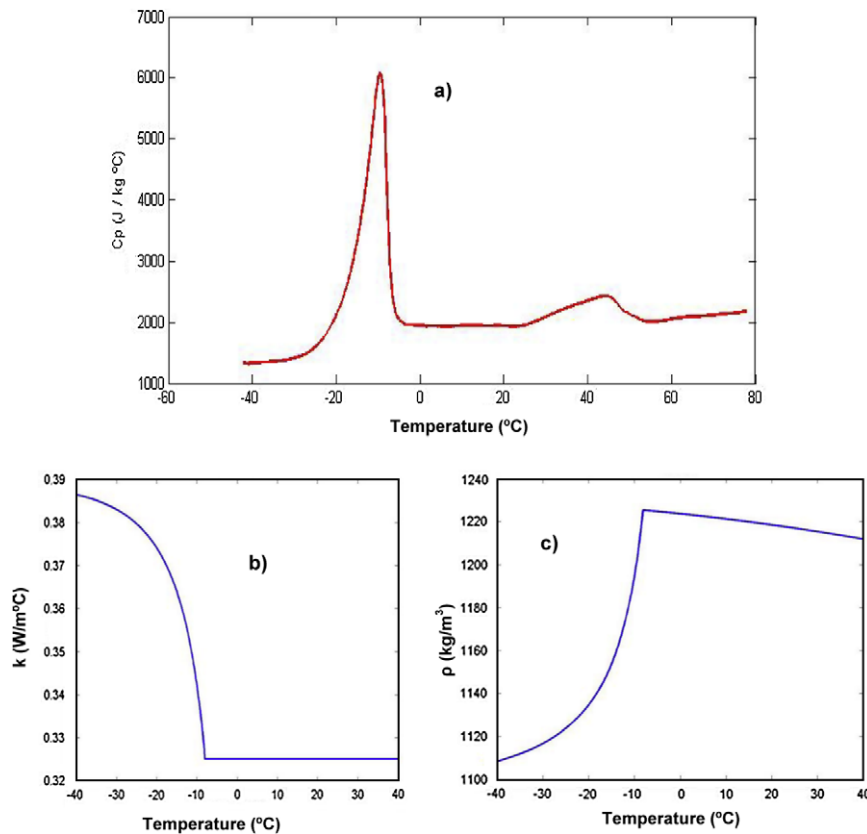


**Fig. 4.** Thermo-physical properties of the bakery product used for the freezing process as a function of temperature (a) specific heat (obtained by DSC), (b) thermal conductivity, (c) density.

temperatures at a symmetry plane of the domain ( $x = 0$ ) with the same chilling residence time.

3.1.4. Application of the numerical model to predict chilling times

The numerical model, once validated and verified experimentally, was used to predict chilling times for different cooling air temperatures (0, 2, 3 °C) and surface heat transfer coefficients, considering a uniform initial product temperature of 20 °C. The time needed to reach 5 °C at the warmest point inside the product was calculated (Table 1). All the numerical runs were tested for their computational speed, the maximum CPU time was 2.3 min using a PC Intel(R) Core(TM) 2 6300 with a processor speed of 1.86 GHz and a RAM of 2 GB.

The implementation of the ODE routine enhanced the computational speed of the code considerably.

3.2. Freezing of irregular 3D bakery products

Fig. 3a shows a digital image of the croissant used in the simulations. The croissants have inherent folds which in all cases are smaller than 1.5 mm in thickness. An interpolating surface was used to smooth these folds, generating a continuous boundary surface which reduced the number of elements and node points needed to create the final mesh. Fig. 3b and c shows the corresponding 3D representation of the irregular shaped body of the croissant and the mesh used to describe the domain.

3.2.1. Thermo-physical properties of the product

The specific heat of the dough (between -40 and 20 °C) including the frozen temperature region, was obtained using the experimental data obtained by DSC (Fig. 4a).

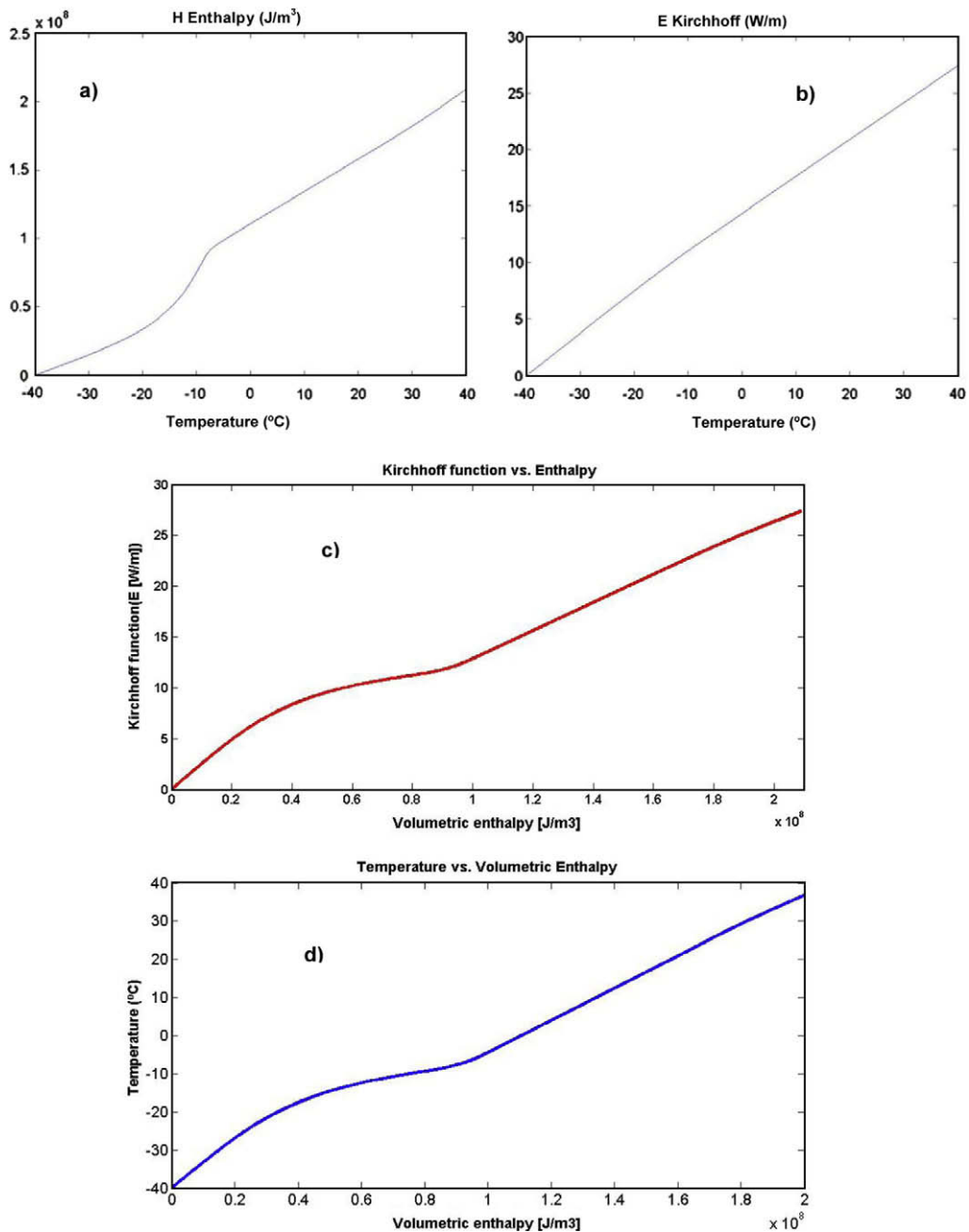


Fig. 5. Functional relationships used in the combined formulation of the freezing process (a) enthalpy vs. temperature, (b) Kirchhoff function vs. temperature, (c) Kirchhoff function vs. enthalpy, (d) temperature vs. enthalpy.



Thermal conductivity of the frozen dough was calculated using the Choi and Okos (1986) equation as follows:

$$k(T) = \sum x_i^v \cdot k_i(T) \quad (25)$$

where  $k$  is the global conductivity,  $k_i$  is the thermal conductivity of the component  $i$  (where  $i$  corresponds to the different components: water, ice if the temperature is lower than the initial freezing temperature  $T_f$ , carbohydrate, fat, etc.),  $x_i^v$  corresponds to the volumetric fraction of each component (Fig. 4b).

The density of the product was calculated using the model proposed by Choi and Okos (1986):

$$\rho(T) = \frac{1}{\sum \frac{x_i}{\rho_i}} \quad (26)$$

where  $\rho(T)$  is the global density and  $\rho_i$  is the density of the component  $i$  (water, carbohydrates, ice, ash, etc.). The fractions “ $x_i$ ” corresponds to the mass fraction of each component (Fig. 4c).

The ice content of the dough as a function temperature (at  $T < T_f$ ) was estimated using the equation proposed by Miles (1974):

$$x_h = (x_w - x_b) \left( 1 - \frac{T_f}{T} \right) \quad (27)$$

where  $x_h$  is the mass fraction of ice,  $T_f$  is the initial melting point of the product,  $x_w$  is the mass fraction of water in the foodstuff, and  $x_b$  is the mass fraction of bound water. The  $x_b$  value was experimentally calculated using the DSC thermogram. The  $x_b$  is related to the ratio between the latent heat of fusion of the food (obtained through integration of the endothermic melting peak) and the latent heat of fusion of water, 333.2 J/g (Weast and Astle, 1981). The  $x_b$  of the dough was 18.4% and this value agrees with published data for un-leavened pastry products (Lind, 1991).

The initial freezing point of the dough obtained from the freezing curves using the tangent method was  $-7.5^\circ\text{C}$ . This value was confirmed by DSC measurements.

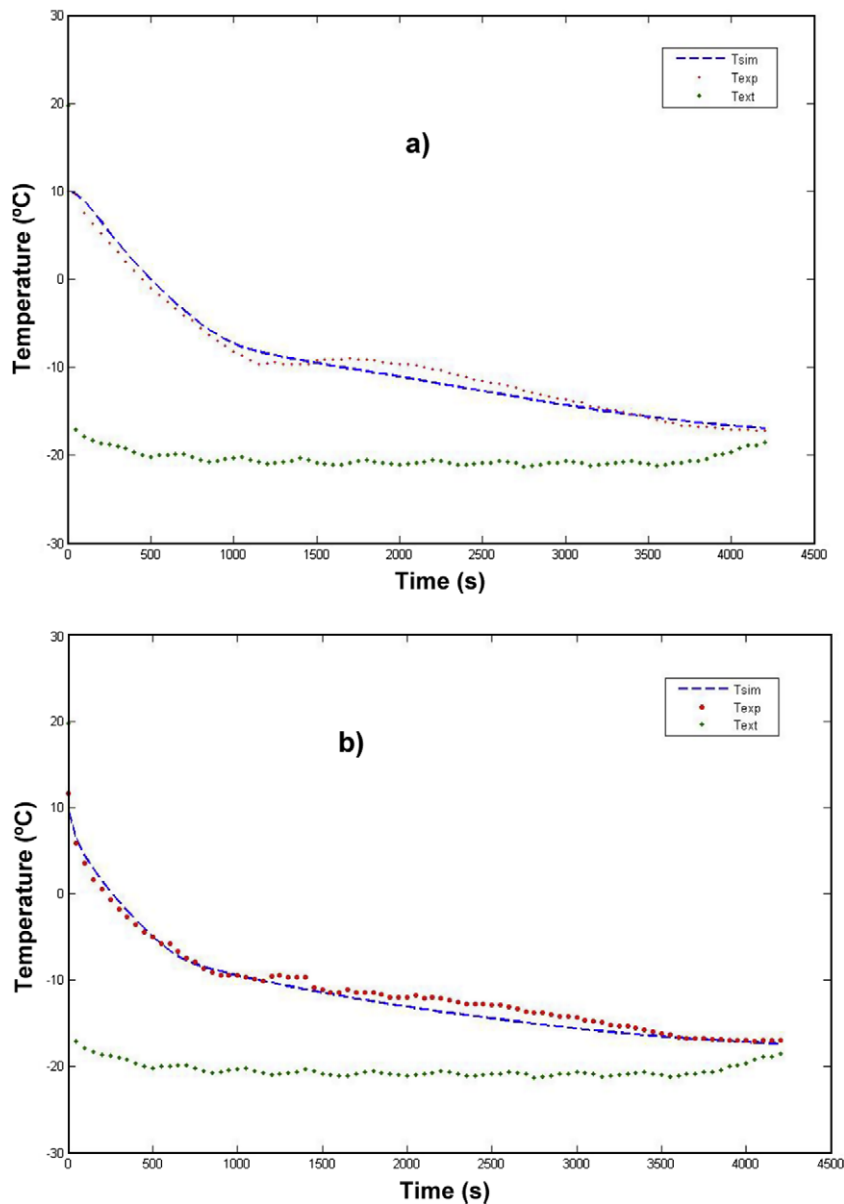


**Fig. 6.** (a) Experimental and predicted temperatures during the freezing process at: (a) the center point of the croissant (point (0, 0, 0)) and (b) a border point given by the following coordinates expressed in meters (0.020, -0.005, 0.010).  $T_{ext} = -20^\circ\text{C}$ ,  $T_i = 10^\circ\text{C}$ . (c) Temperature distribution of the croissant after 25 min residence time in the tunnel freezer ( $h = 18 \text{ W/m}^2 \text{ }^\circ\text{C}$ ,  $T_i = 10^\circ\text{C}$ ) (a) at the surface (d) at a symmetry plane.

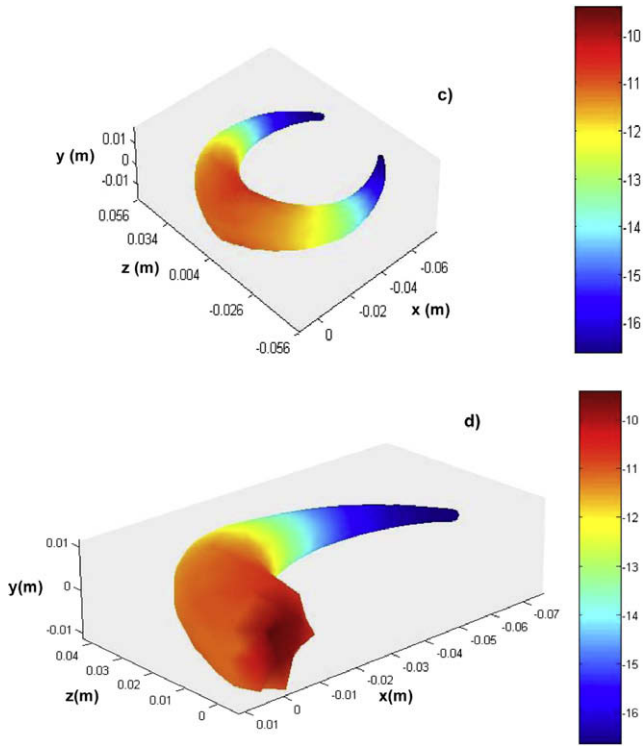


Fig. 6 (continued)

The volumetric specific heat in Eq. (10) was obtained by multiplying the  $\rho(T)$  by the  $C_p(T)$ , and further numerically integrated using Eq. (11) to obtain the enthalpy function (Fig. 5a). The same procedure was carried out with the  $k(T)$  in order to obtain the Kirchhoff function ( $E(T)$ ) according to Eq. (12) (Fig. 5b). Fig. 5c and d shows the functions  $E(H)$  and  $T(H)$ , respectively.

3.2.2. Surface heat transfer coefficient

The heat transfer coefficient ( $h$ ) was determined from the experiments performed using the acrylic prototype placed in the tunnel freezer at  $(-20\text{ }^\circ\text{C})$ ; the average value of  $h$  that minimized the RSS in Eq. (23) was  $18\text{ W/m}^2\text{ }^\circ\text{C}$ .

The  $h$  value for solid objects immersed in fluids under forced convection conditions, was also estimated using correlations found in literature which take into account the  $Nu = hL/k$ ,  $Re = \rho vL/\mu$ , and  $Pr = Cp\mu/k$  numbers (Earle, 1988) as follows:

$$Nu = 0.036 \cdot (Re)^{0.8} (Pr)^{0.33} \quad \text{for } Re > 2 \times 10^4 \quad (28)$$

The value of air velocity in the tunnel freezer was  $2.5\text{ m/s}$ . In order to estimate the characteristic length of the croissant used in the  $Re$  number, the average between the maximum distance in the  $x$  and  $y$  direction of the irregular shaped body was adopted,  $L = 8.75\text{ cm}$ . The value of  $h$  obtained by applying Eq. (28) was  $20.80\text{ W/m}^2\text{ }^\circ\text{C}$ .

A simple equation valid for the case in which the fluid is air, considering velocities lower than  $5\text{ m/s}$  was also applied (Earle, 1988):

$$h = 5.7 + 3.9 \cdot v \quad (29)$$

The obtained value of  $h$  from Eq. (29) was  $15.5\text{ W/m}^2\text{ }^\circ\text{C}$ ; therefore it can be observed that the value estimated through the transient method ( $18\text{ W/m}^2\text{ }^\circ\text{C}$ ) is in the range of the  $h$  values estimated by literature correlations.

Table 2

Freezing times (min) for different values of  $T_{ext}$  and  $h$  (surface heat transfer coefficient).

$T_{ext}$ ( $^\circ\text{C}$ )	Surface heat transfer coefficient $h$ ( $\text{W/m}^2\text{ }^\circ\text{C}$ )					
	5	10	15	20	40	50
-30	85.5	47.0	33.8	27.0	16.8	14.8
-35	69.0	38.0	27.3	22.0	13.8	12.2
-40	58.3	32.3	23.3	18.8	11.8	10.5

3.2.3. Comparison of the numerical model with experimental results for the freezing process

The numerical code implementing the Enthalpy and Kirchhoff transformations was compared with experimental freezing curves found in literature for irregular minced meat objects containing 75% water (Cleland et al., 1987a,b; Califano and Zartzky, 1997). The numerical predictions resulted in agreement with the experimental data, even though the material exhibited a sharp phase change.

Additionally, the numerical simulations obtained with the code, were contrasted with experimental time–temperature freezing curves of 3D objects (croissants). The process was carried out in a tunnel freezer at a temperature of  $-20\text{ }^\circ\text{C}$ , with an air velocity  $v = 2.5\text{ m/s}$ ; the surface heat transfer coefficient  $h$  was  $18\text{ W/m}^2\text{ }^\circ\text{C}$ .

Fig. 6a and b shows the predicted and experimental temperatures at the center and a border point of the croissant obtained for the different freezing experiments. As can be seen the numerical model satisfactorily predicts the time–temperature evolution of the freezing process. For all the tested cases the absolute value of the maximum difference between the predicted and experimental temperatures (infinite norm of the error) was less than  $1.7\text{ }^\circ\text{C}$ . Fig. 6c shows the temperature distribution after 25 min inside the tunnel freezer and Fig. 6d the temperature distribution at the symmetry plane of the irregular shape body. It can be observed that the flattened ends of the croissant reached lower temperatures much faster than the thicker central zone.

3.2.4. Application of the numerical model to predict freezing times

Simulations were carried out in order to obtain the freezing times for different external fluid temperatures and surface heat transfer coefficients values, considering an initial temperature of  $10\text{ }^\circ\text{C}$ . The time needed to reach a value of  $-18\text{ }^\circ\text{C}$  in the warmest point of the croissant was calculated (Table 2).

The numerical runs were tested for their computational speed with the same computer. The CPU time needed to simulate the freezing process was less than 3 min for the numerical runs. It is noteworthy that the computational speed of the numerical simulations of the freezing process is comparable to the chilling process, due to the simultaneous Kirchhoff and enthalpy transformation. Using this combined transformation the conductance, capacitance, and convective matrices as well as the thermal load vector in the finite element formulation remained independent of the time variable.

4. Conclusions

Robust finite element codes for irregular 3D food systems, were developed by the authors, to simulate the chilling process considering domains of different thermo-physical properties, as well as the freezing operation using a combined enthalpy and Kirchhoff transformation.

The irregular 3D geometry was taken into account using CAD files to generate the spatial discretization of the domain.

The specific heats of the food materials were measured using Differential Scanning Calorimetry and the heat transfer coefficients

of the low temperature equipments were determined; this information was further used as inputs in the numerical code.

The numerical code for chilling was validated using analytical solutions and the simulations were compared with experimental time–temperature data of a semi-elaborated heterogeneous bakery product (“empanada” or Cornish pastry) chilled in a cold chamber.

For the freezing process a 3D finite element code using a combined enthalpy and Kirchhoff transformation method was implemented. The simulations obtained by the numerical codes were compared to results published in the literature and to experimental data of croissants frozen in a tunnel.

A good agreement between experimental temperatures and numerical predictions were obtained in all cases (chilling and freezing).

It is important to remark that in the complex freezing process the application of the enthalpy–Kirchhoff formulation decreased the computational efforts improving the rate of convergence and the execution speed with respect to the commercial softwares.

The codes were finally applied to determine the required time–temperature conditions for food cooling and freezing.

## Acknowledgements

The authors acknowledge the financial support provided by the Consejo Nacional de Investigaciones Científicas y Tecnológicas (CONICET), Agencia Nacional de Promoción Científica y Tecnológica (ANPCYT), and Universidad Nacional de La Plata, Argentina.

## References

- Arce, J.A., Potluri, P.L., Schneider, K.C., Sweat, V.E., Dutson, T.R., 1983. Modeling Beef carcasses cooling using finite element technique. *Transactions of the ASAE* 26, 950–954, 960.
- ASTM Standard E1269-05, 2003. Standard Test Method for Determining Specific Heat Capacity by Differential Scanning Calorimetry. ASTM International, West Conshohocken, PA. doi:10.1520/E1269-05. <www.astm.org>.
- Baik, O.D., Marcotte, M., Sabiani, S.S., Castaigne, F., 2001. Thermal and physical properties of bakery products. *Critical Reviews in Food Science and Nutrition* 41 (5), 321–352.
- Bathe, K.J., 1996. *Finite Element Procedures*. Prentice Hall Inc., Englewoods Cliff, New Jersey.
- Califano, A., Zaritzky, N., 1997. Simulation of freezing or thawing heat conduction in irregular two dimensional domains by a boundary fitted grid method. *Lebensmittel-Wissenschaft und-Technologie* 30, 70–76.
- Carslaw, H.S., Jaeger, J.C., 1959. *Conduction of Heat in Solids*. University Press, Oxford.
- Choi, Y., Okos, M.R., 1986. Effects of temperature and composition on the thermal properties of foods. In: Le Maguer, M., Jelen, P. (Eds.), *Food Engineering and Process Applications*, vol. 1. Elsevier Applied Science, New York, pp. 93–103.
- Cleland, D.J., Cleland, A.C., Earle, R.L., Byrne, S.J., 1984. Prediction of rates of freezing, thawing or cooling in solids of arbitrary shape using the finite element method. *International Journal of Refrigeration* 7 (1), 6–13.
- Cleland, D.J., Cleland, A.C., Earle, R.L., Byrne, S.J., 1987a. Prediction of freezing and thawing times for multi-dimensional shapes by numerical methods. *International Journal of Refrigeration* 10, 32–39.
- Cleland, D.J., Cleland, A.C., Earle, R.L., Byrne, S.J., 1987b. Experimental data for freezing and thawing of multi-dimensional objects. *International Journal of Refrigeration* 10, 22–31.
- Comini, G., Del Giudice, S., Lewis, R.W., Zienkiewicz, O.C., 1974. Finite element solution of non-linear heat conduction problems with special reference to phase change. *International Journal for Numerical Methods in Engineering* 8, 613–624.
- Comini, G., Nonino, C., Saro, O., 1990. Performance of enthalpy-based algorithms for isothermal phase change. *Advanced Computational Methods in Heat Transfer, Phase Change and Combustion Simulation* 3, 3–13.
- Earle, R.L., 1988. *Ingeniería de los alimentos*, second ed. Acribia, Zaragoza.
- Fennema, O.R., Powrie, W.D., Marth, E.H., 1973. *Low Temperatures Preservation of Foods and Living Matter*. Marcel Dekker Inc., New York.
- Fikiin, K.A., 1996. Generalized numerical modeling of unsteady heat transfer during cooling and freezing using an improved enthalpy method and quasi-one-dimensional formulation. *International Journal of Refrigeration* 19 (2), 132–140.
- Fikiin, K.A., 1998. Some general principles in modeling of unsteady heat transfer in two-phase multi-component aqueous food systems for product quality improvement. In: Nicolai, B.M., De Baerdemaeker, J. (Eds.), *Food Quality Modelling*. Office for Official Publications of the European Communities, Luxembourg, pp. 179–186.
- Le Bail, A., Goff, H.D., 2008. Freezing of bakery and dessert products. In: Evans, J. (Ed.), *Frozen Food Science and Technology*. Blackwell Publishing, Oxford, pp. 184–203.
- Lind, I., 1991. The measurement and prediction of thermal properties of food during freezing and thawing – a review with particular reference to meat and dough. *Journal of Food Engineering* 13, 285–319.
- Lorenzo, G., Zaritzky, E.N., Califano, A.N., 2009. Rheological characterization of refrigerated and frozen non-fermented gluten-free dough: effect of hydrocolloids and lipid phase. *Journal of Cereal Science* 50, 255–261.
- Mannapperuma, J.D., Singh, R.P., 1988. Prediction of freezing and thawing times of foods using a numerical method based on enthalpy formulation. *Journal of Food Science* 53, 626–630.
- Mannapperuma, J.D., Singh, R.P., 1989. A computer-aided method for prediction of properties and freezing/thawing times of foods. *Journal of Food Engineering* 9, 275–304.
- McNaughton, J.L., Mortimer, C.T., 1975. *Calorimetría diferencial de barrido*. Perking Elmer Corporation, Connecticut.
- Miles, C.A., 1974. The ice content of frozen meat and its measurements using ultrasonic waves. In: Cutting (Ed.), *Meat Freezing: Why and How*. AFRC Meat Research Institute, Oxford, pp. 151–157.
- Nesvadba, P., 2008. Thermal properties and ice crystal development in frozen foods. In: Evans, J. (Ed.), *Frozen Food Science and Technology*. Blackwell Publishing, Oxford, pp. 1–25.
- Pham, Q.T., 2008. Modelling of freezing processes. In: Evans, J. (Ed.), *Frozen Food Science and Technology*. Blackwell Publishing, Oxford, pp. 51–80.
- Rahman, M.S., Sablani, S.S., Al-Habsi, N., Al-Belushi, R., 2005. State diagram of freeze-dried garlic powder by differential scanning calorimetry and cooling curve methods. *Journal of Food Science* 70 (2), 135–141.
- Ribotta, P.D., León, A.E., Añón, M.C., 2006. Frozen dough. In: Hui, Y.H. (Ed.), *Baked Products*. Science and Technology. Blackwell Publishing, Oxford, pp. 381–390.
- Santos, M.V., Zaritzky, N., Califano, A., Vampa, V., 2008. Numerical Simulation of the Heat Transfer in Three Dimensional Geometries. *Mecánica Computacional*, vol. XXVII, no. 21. Heat Transfer (C) Ed. Asociación Argentina de Mecánica Computacional (AMCA), pp. 1705–1718.
- Scheerlinck, N., Fikiin, K.A., Verboven, P., DeBaerdemaeker, J., Nicolai, B.M., 1997. Numerical solution of phase change heat transfer problems with moving boundaries using an improved finite element enthalpy method. In: Van Keer, R., Brebbia, C.A. (Eds.), *Moving Boundaries IV: Computational Modelling of Free and Moving Boundary Problems*. pp. 75–85.
- Scheerlinck, N., Verboven, P., Fikiin, K.A., De Baerdemaeker, J., Nicolai, B.M., 2001. Finite element computation of unsteady phase change heat transfer during freezing or thawing of food using a combined enthalpy and Kirchhoff transform method. *Transactions of the ASAE* 44 (2), 429–438.
- Shampine, L.F., Reichelt, M.W., 1997. The matlab ODE suite. *SIAM Journal on Scientific Computing* 18 (1), 1–22.
- Sweat, V.E., 1975. Modeling the thermal conductivity of meats. *Transactions of the ASAE* 18 (3), 564–568.
- Weast, R.C., Astle, M.J., 1981. *Handbook of Chemistry and Physics*, 63rd ed. CRC press, Florida, Boca Raton.
- Welty, J.R., 1974. *Engineering Heat Transfer*. John Wiley & Sons, New York.
- Zienkiewicz, O.C., Taylor, R.L., 1994a. *El método de los elementos finitos*, vol. I. McGraw-Hill, Barcelona.
- Zienkiewicz, O.C., Taylor, R.L., 1994b. *El método de los elementos finitos*, vol. II. McGraw-Hill, Barcelona.